

COMPUTATIONAL MODELLING OF RESIDUAL STRESS EFFECTS ON CRACK INITIATION AND GROWTH IN DUCTILE MATERIALS

Noel P. O'Dowd, Yuebao Lei, Philip S. May and George A. Webster

Department of Mechanical Engineering
Imperial College, London, SW7 2BX, UK

ABSTRACT

In this work the effect of residual stress on fracture initiation and growth is examined numerically. A void growth and coalescence model is used to simulate the effect of local damage in the vicinity of a crack in a ductile material. It is seen that, for the cases examined, a J -based characterisation of the crack growth is still appropriate when residual stresses are present. The significance of the effect of residual stress on crack growth is examined for two material ductilities.

KEYWORDS

Fracture; residual stress; J -integral; finite element analysis.

INTRODUCTION

The J -integral has been adopted by most current structural integrity procedures for cracked bodies under combined secondary and primary loadings, *e.g.* R6 [?], BS 7910 [?] and EPRI [?] methods. The implicit assumption when applying these approaches is that the effect of the residual stresses may be accounted for through modification of the driving force, J , and the inherent toughness of the material remains unchanged. However, this assumption may not be valid in view of the well known effect of stress state (constraint) on the fracture toughness of materials, *e.g.* [?]. In this paper a numerical study is carried out to assess the influence of residual stress on the fracture of a ductile ferritic steel.

COMPUTATIONAL FRAMEWORK

A finite element analysis of a three point bend testing configuration is undertaken. The analyses have been carried out using the commercial finite element code ABAQUS V5.8 [?]. Full account is taken of material and geometric non-linearities with the resultant non-linear equilibrium equations being solved iteratively using Newton's method (see [?]). A typical finite element mesh, which is composed of about 2000 four noded isoparametric quadrilaterals, is shown in Fig. 1. Due to symmetry only half of the problem is analysed. The failure mechanism examined is that of void growth and coalescence, which is incorporated into the model using a Gurson-type failure model, developed for porous materials, ([?],

[?]). Within this model, the yield surface of the material, Φ , is a function of the evolving void volume fraction f ,

$$\Phi = \left(\frac{\sigma_e}{\sigma_y}\right)^2 + 2q_1 f \cosh\left(-q_2 \frac{3p}{2\sigma_y}\right) - (1 + q_1^2 f^2) = 0, \quad (1)$$

where σ_e is the equivalent stress, p the hydrostatic pressure and σ_y the yield stress of void-free material. The material parameters q_1 and q_2 depend on the hardening exponent n and on the ratio E/σ_y , where E is the Young's modulus [?].

The void growth rate is expressed in terms of the current value of f and the plastic strain rate tensor $\dot{\epsilon}^P$ as

$$\dot{f} = (1 - f) \dot{\epsilon}^P : \mathbf{I}, \quad (2)$$

where \mathbf{I} is the second order unit tensor. Finally, to completely define the material softening behaviour, the critical void volume fraction, f_e , at which the stress carrying capacity of the material is lost must also be specified. Once the void volume fraction, f , at a material point reaches this value, the stiffness at that point is gradually reduced to zero and the element is then removed from the analysis. If the removed element is directly ahead of the crack tip, the crack is considered to have grown by an amount equal to the element size. As seen in Fig. 1(b), ahead of the initial crack tip the finite element mesh consists of regular square elements. The use of an element removal approach to simulate crack growth introduces as an additional length scale into the problem, the size of these crack tip elements (see, *e.g.*, [?]). This characteristic length scale (*i.e.*, local mesh size) should be associated with a physically meaningful quantity such as the mean inclusion spacing or the CTOD of the material [?].

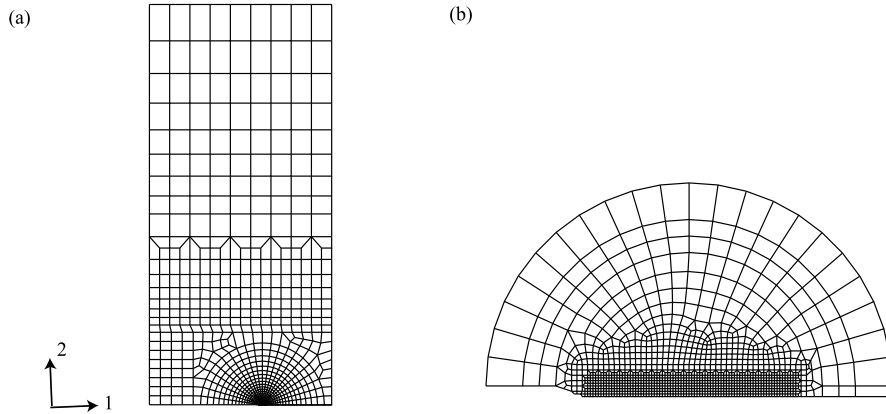


Figure 1: Finite element mesh used in the analysis (a) full mesh (b) near tip region

Evaluation of J integral

The evaluation of a path independent J integral value in the presence of residual stress has been discussed in [?]. A path independent J -integral equation can be obtained via,

$$J = \int_{\Gamma} \left(W \delta_{1i} - \sigma_{ij} \frac{\partial u_j}{\partial x_1} \right) n_i ds; + \int_A \sigma_{ij} \frac{\partial \epsilon_{ij}^0}{\partial X_1} dA, \quad (3)$$

where A is the area enclosed within a contour Γ and W is the mechanical strain energy density,

$$W = \int_0^{\epsilon_{ij}^m} \sigma_{ij} d\epsilon_{ij}^m. \quad (4)$$

Note that $A \rightarrow 0$ as $\Gamma \rightarrow 0$ and implicit in this definition for J is the assumption that the initial strains, ϵ_{ij}^0 , are bounded at the crack tip, [?].

The initial strains, ϵ_{ij}^0 in Eq. 3, are determined as the difference between the total strains and the elastic mechanical strains at the initial state, *i.e.*

$$0 = (\epsilon_{ij}^0) \quad (5)$$

In this work, the residual stress in the specimen, before a crack has been introduced, is assumed to be available. This residual stress is then introduced into the finite element model as an initial condition and the effect of introducing a crack is represented by the removal of the symmetry boundary conditions along the crack plane (see [?]). The initial state, at which ϵ^0 is evaluated, is then the state after the initial residual stress is input, before the crack is introduced. This procedure has been shown to provide a path independent integral and, for linear elastic behaviour, results for J consistent with those obtained using linear superposition, [?]. In this analysis, to avoid loss of path independence on contours near to the growing crack tip, only the outer rings in the finite element mesh are used in the evaluation of J (outside the fine square mesh region illustrated in Fig. 1 (b)).

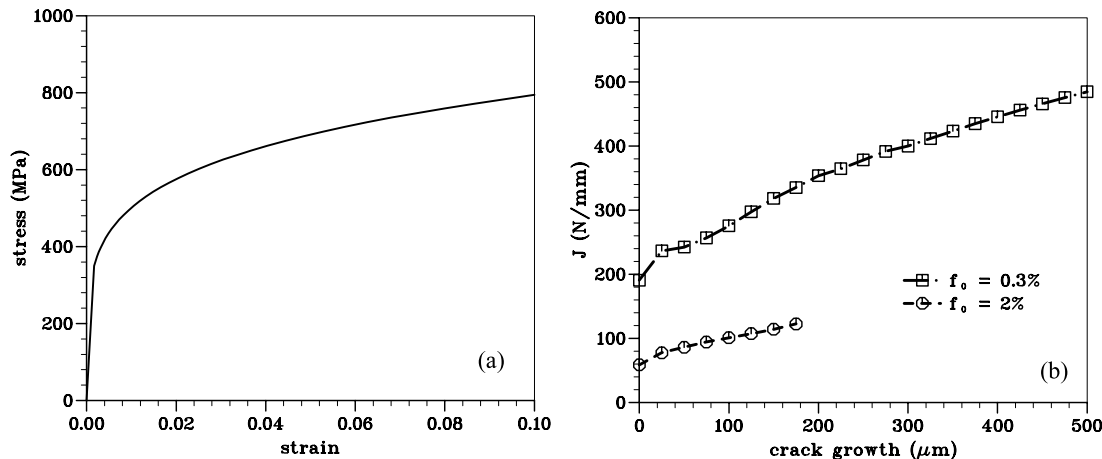


Figure 2: (a) Uniaxial stress-strain behaviour of the material (b) J -resistance curves with two values of initial void volume fraction, f_0

MATERIAL AND SPECIMEN PROPERTIES

The uniaxial stress-strain behaviour of the material is shown in Fig. 2(a). This behaviour is representative of a low strength offshore steel (BS 7191 Grade 355 EMZ), which is being studied as part of a larger overall program. The material has a yield strength of 350 MPa and the post yield strain hardening is represented here as a power law with $n = 5$.

The values of q_1 and q_2 related to the mechanics of void growth in Eq. 1 have been taken from [?] and are given by $q_1 = 2.0$ and $q_2 = 0.8$, respectively. The mesh size, D , (twice the size of the square elements in the crack tip region) used in the crack growth calculations is taken as $50 \mu\text{m}$ which is on the order of the measured CTOD for the BS 7191 Grade 355 EMZ steel. The sensitivity of the results to the mesh size is currently under investigation. The critical void volume fraction f_e is taken to be 10%.

The effect of the initial void volume fraction, f_0 on the predicted resistance curve behaviour is shown in Fig. 2(b). These results were determined from a study of a three point bend geometry with overall specimen width, W , of 50 mm and initial crack size, a , of 30 mm. The high toughness material with $f_0 = 0.3\%$ is representative of the toughness of the ferritic steel, (BS 7191 Grade 355 EMZ) at room temperature. The strong effect of f_0 is noted by comparison with the predicted resistance curve behaviour when $f_0 = 2\%$. Note that both materials have the same uniaxial stress strain behaviour, shown in Fig. 2(a). The analysis for $f_0 = 2\%$ terminates at $\Delta a = 200 \mu\text{m}$ due to numerical difficulties. However, the trend of the behaviour is clear, even at this amount of crack growth.

EFFECT OF RESIDUAL STRESS ON RESISTANCE CURVE BEHAVIOUR

A representative residual stress distribution is examined in this paper. Future work will present results for measured residual stress distributions due to welding, [?]. The distribution examined is shown in Fig. 2 and the effect of the residual stress on the resistance curve behaviour is examined.

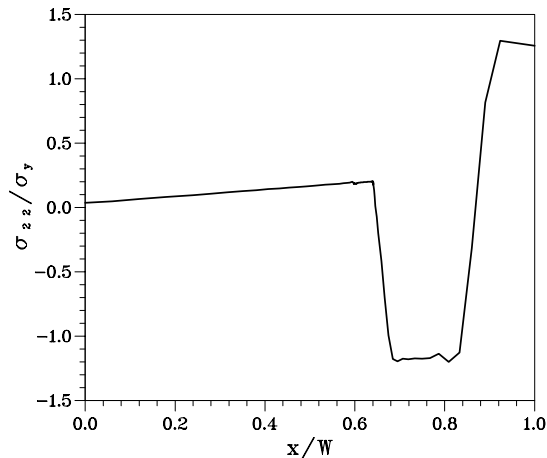


Figure 3: Residual stress distribution used in the analysis.

is shown. The value of a/W for the three point bend geometry is 0.6 so the crack tip is located at $x/W = 0.6$. This residual stress profile was chosen to provide a reasonably high fracture driving force due to residual stress. Note that, despite the fact that the uncracked body residual stress shown in Fig. 3 is close to zero along the crack faces, the J value due to the residual stress field determined from the finite element analysis is still significant (11 N/mm).

The resultant load *vs.* crack growth curves are shown in Figs. 4 (a) and (b) for the two material toughnesses. It is seen that for the high toughness material (Fig. 4(a)), there is a very small effect of residual stress on the load to cause crack initiation, (note that the J value due to residual stress is less than 1% of the initiation J) and after some crack growth, this effect almost disappears. For the low toughness material, Fig. 4(b), however, there is a strong effect of residual stress on the initiation load, though again the effect diminishes somewhat after crack growth. For the low toughness material, the load corresponding to $\Delta a = 50\mu$ m is about 20% lower when residual stresses are present. In Figs. 4(c) and (d) the J -resistance curves with and without residual stress are shown for the two materials examined. For the high toughness material (Fig. 4(c)), the resistance curves are almost indistinguishable. For the low toughness material (Fig. 4(d)), there is a small difference (maximum of 8%) between the resistance curves—the J resistance curve is slightly higher for the specimen with residual stress. If it is assumed that J retains its validity as a fracture parameter when residual stresses are present, any effects on the J resistance curve must be accounted through constraint arguments—the loss of J dominance in the specimen. At higher loads the effect of the residual stress is expected to diminish as the deformation is controlled by the applied mechanical load. Therefore constraint effects are expected to be more significant for lower strength materials as indeed is observed here. Similar trends have been observed in [?] where it was found that residual stress had a strong effect on the onset of brittle fracture but a much reduced effect on ductile fracture.

DISCUSSION AND CONCLUSIONS

The effect of residual stress on the fracture behaviour of a high and low toughness material have been examined numerically. A Gurson-type void growth model has been used to simulate the effect of damage ahead of a growing crack tip. It is seen that the $J - \Delta a$ behaviour of the material is relatively unaffected by the existence of the residual stress field for both materials. The damage introduced by the residual stress near the crack tip, is well accounted for by the use of J as the driving force for fracture. This implies that when residual stresses are present, it is acceptable to incorporate the residual stresses into the driving force and to assume that the material resistance is unaffected.

The geometry examined is a high constraint three point bend geometry and the residual stress field examined has a relatively low J and associated T stress. Different geometrical configurations, materials and residual stress distributions may lead to different results from those presented here. It should also

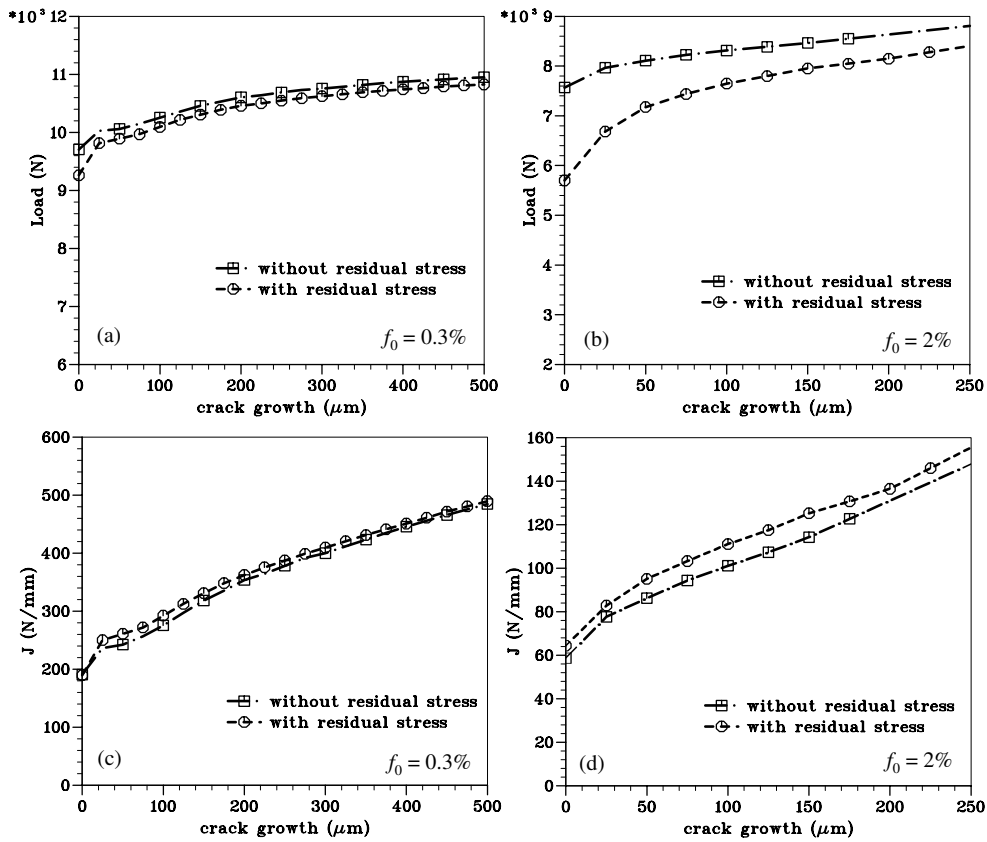


Figure 4: (a) and (b) Load vs crack growth for (a) high toughness material, (b) low toughness material; (c) and (d) J -resistance curves for (c) high toughness material and (d) low toughness material.

be pointed out that if the residual stress has been introduced due to welding or by a heat treatment there may be some effect on the material microstructure, in which case the intrinsic toughness of the material may change. Such effects have not been examined in this analysis.

ACKNOWLEDGMENTS

Financial support for this work, provided by the IMC, HSE, EPSRC and DERA, is gratefully acknowledged.

References

- [1] British Energy Generation Ltd. (1998) Assessment of the Integrity of Structures Containing Defects, R/H/R6-Revision 3.
- [2] British Standards Institution, 2001, Guidance on Methods for Assessing the Acceptability of Flaws in Welded Structures, BS7910, London, UK.
- [3] Kumar, V., Schumacher, B. I. and German, M. D. (1984) Development of a procedure for incorporation secondary stress in the engineering approach, in *EPRI Report EPRI NP-3607*.
- [4] O'Dowd, N. P. (1995) *Engng. Frac. Mechanics* **52** 3, 445.
- [5] ABAQUS/STANDARD V. 5.8 (1999), Hibbitt, Karlsson and Sorensen Inc., Providence, RI.
- [6] Gurson, A. L. (1977) *J. Engng. Mat. Tech.* **99** 2.
- [7] Tyorgaard V. (1990) *Advances in Applied Mechanics* **27** 83.

- [8] Faleskog, J., Gao, X. and Shih, C. F. (1998) *Int. J. Fracture* **89** 4, 355.
- [9] Xia, L. and Shih, C.F. (1995) *J. Mech. Phys. Sol.*, **43**, 233.
- [10] Lei, Y., O'Dowd, N. P. and Webster, G. A. (2000) *Int. J. Fracture* **106** 195.
- [11] Ainsworth, R. A., Neale, B. K. and Price, R. H. (1978) In: *Proc. Int. Conf. on Tolerance of Flaws in Pressurised Components*, 171.
- [12] May, P., Lei, Y., Webster, G. A., O'Dowd, N. P. (1998) Investigation of residual stresses in welded joints, Imperial College report, REF: MESMPN0228/MESMPR0374.
- [13] Panontin, T.L and Hill, M.R. (1996) *Int. J. Fracture* **82** 317.